Electrochemical investigation of the hydrogen evolution reaction on electrodeposited films of $Cr(OH)_3$ and Cr_2O_3 in mild alkaline solutions

Adriano S. O. Gomes[1,2], Nina Simic[2], Mats Wildlock[2], Anna Martinelli[3], Elisabet Ahlberg[1,*]
[1]Department of Chemistry and Molecular Biology, University of Gothenburg, Kemigården 4, SE-412 96 Gothenburg, Sweden
[2]AkzoNobel Pulp and Performance Chemicals, SE-445 80 Bohus, Sweden
[3]Department of Chemistry and Chemical Engineering, Chalmers University of Technology, Kemigården 4, SE-412 96 Gothenburg, Sweden

*ela@chem.gu.se

Supporting information

Raman spectra from different spots of a $Cr(OH)_3$@Ti electrode analysed using 3.5 mW laser power are compiled in Figure S1. It is generally observed that most of the $Cr(OH)_3$ was converted to Cr_2O_3, since the signatures characteristic for crystalline Cr_2O_3 are observed. However, in the spectra taken from spots 1 and 5, the broad band at 850 cm^{-1}, related to $Cr(OH)_3$, can still be observed. Spots 2, 3 and 4, show only the sharp peak at ~550 cm^{-1} that can be assigned to Cr_2O_3, the other bands are related with the Ti substrate, showing the thickness of the $Cr(OH)_3$ film in these spots was very thin (or thinner than in spots 1 and 5).

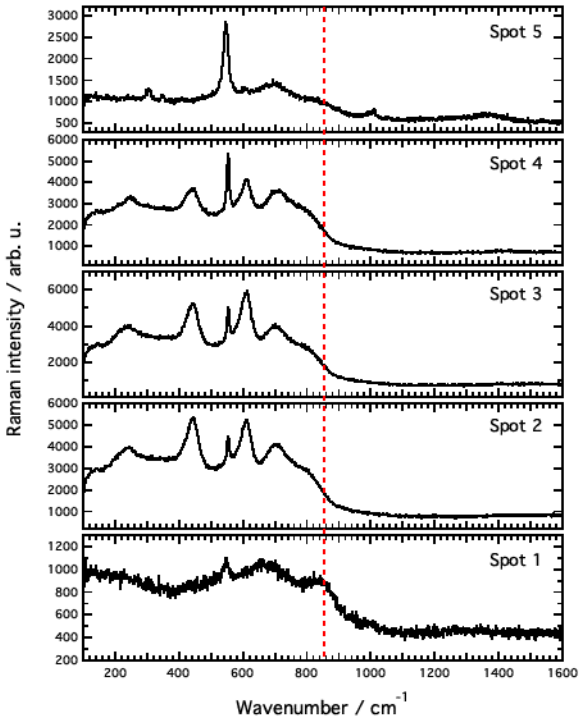

Figure S1 – Raman spectra of $Cr(OH)_3$@Ti taken at five different spots on the surface, using a laser power of 3.5 mW.

X-ray diffraction (XRD) was performed on a Siemens D5000 Diffractometer with a Bragg-Brentano set up equipped with a Cu k_α X-Ray source and a scintillation detector at 0.100º intervals of 2θ, and cumulated count time of 4 s for each step. The grazing angle setup was used at 4º. The diffractograms obtained for both $Cr(OH)_3$@Ti and Cr_2O_3@Ti are depicted in Figure S2a and Figure S2b, respectively. In both cases, no diffraction peaks related to Cr(III) were observed. Other grazing angles ranging from 2º to 10º were also investigated with no dramatic changes observed, comparing to results presented in Figure S2. $Cr(OH)_3$ is known to be XRD amorphous, and therefore it was not strange that no diffraction peaks were observed other than Ti. Cr_2O_3, on the other hand, is usually crystalline in XRD and the peaks obtained were compared with Cr_2O_3 indexed values (PDF 00-006-0504), but no correlations were observed. The differences in intensities can be explained by the thickness of the Cr(III) films. $Cr(OH)_3$ is thinner than Cr_2O_3, and more signals from the substrate were detected. In the case of Cr_2O_3, signals from Ti are so weak that other peaks are covered by the intrinsic noise of the measurement.

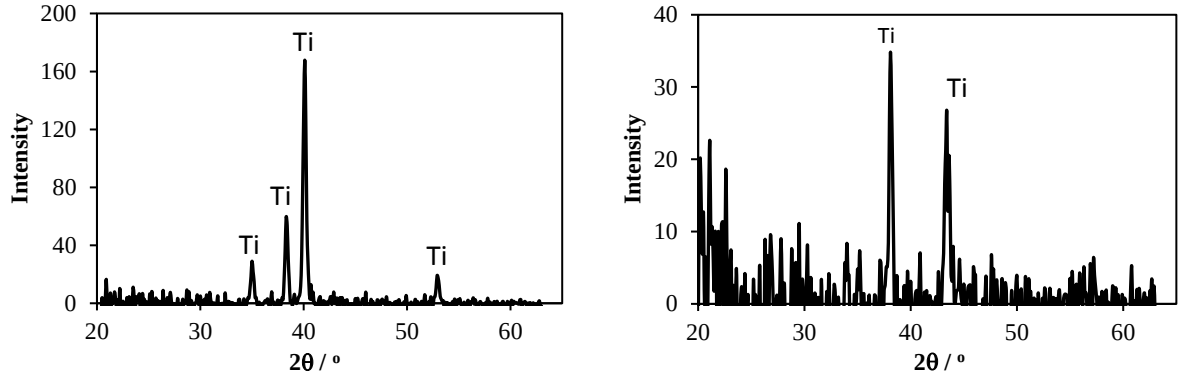

Figure S2 – Diffractograms of Ti RDE covered with (a) $Cr(OH)_3$ and (b) Cr_2O_3.

The composition of the outmost layer of the $Cr(OH)_3$@Ti and Cr_2O_3@Ti electrodes were analysed by X-Ray Photoelectron Spectroscopy (XPS) on a PHI 5000C ESCA System (Perkin Elmer). The monochromatic Al K_α was used as X-ray source ($h\nu$ = 1486.7 eV). Cr2p and O1s peak positions were adjusted with respect to the C1s background/impurity on the sample and the peaks were fitted in Origin Lab© 8.1. Analyses of the XPS data was hampered by the bad quality of the C1s peak used to calibrate the curves (Figure S3a and FigureS3b). The peak was fitted with two Gaussians, and the highest peak was centred at 285.5 eV. Then, the peaks positions for the O1s, Cr2p3/2p and Cr2p1/2 were adjusted accordingly, and are presented in Figure S3c-S3f. The positions for the most intense peaks are given in Table S1, together with literatures values for $Cr(OH)_3$, Cr_2O_3 and metallic Cr. Figures S3e shows that four peaks were necessary to fit the experimental data. The two extra peaks centred at 575.5 and 585.3 eV are close to Cr^0 literature values, and the presence of this species cannot be neglected. In Figure S3f, six peaks were necessary to fit the whole data, indicating formation of a more complex Cr_2O_3 matrix.

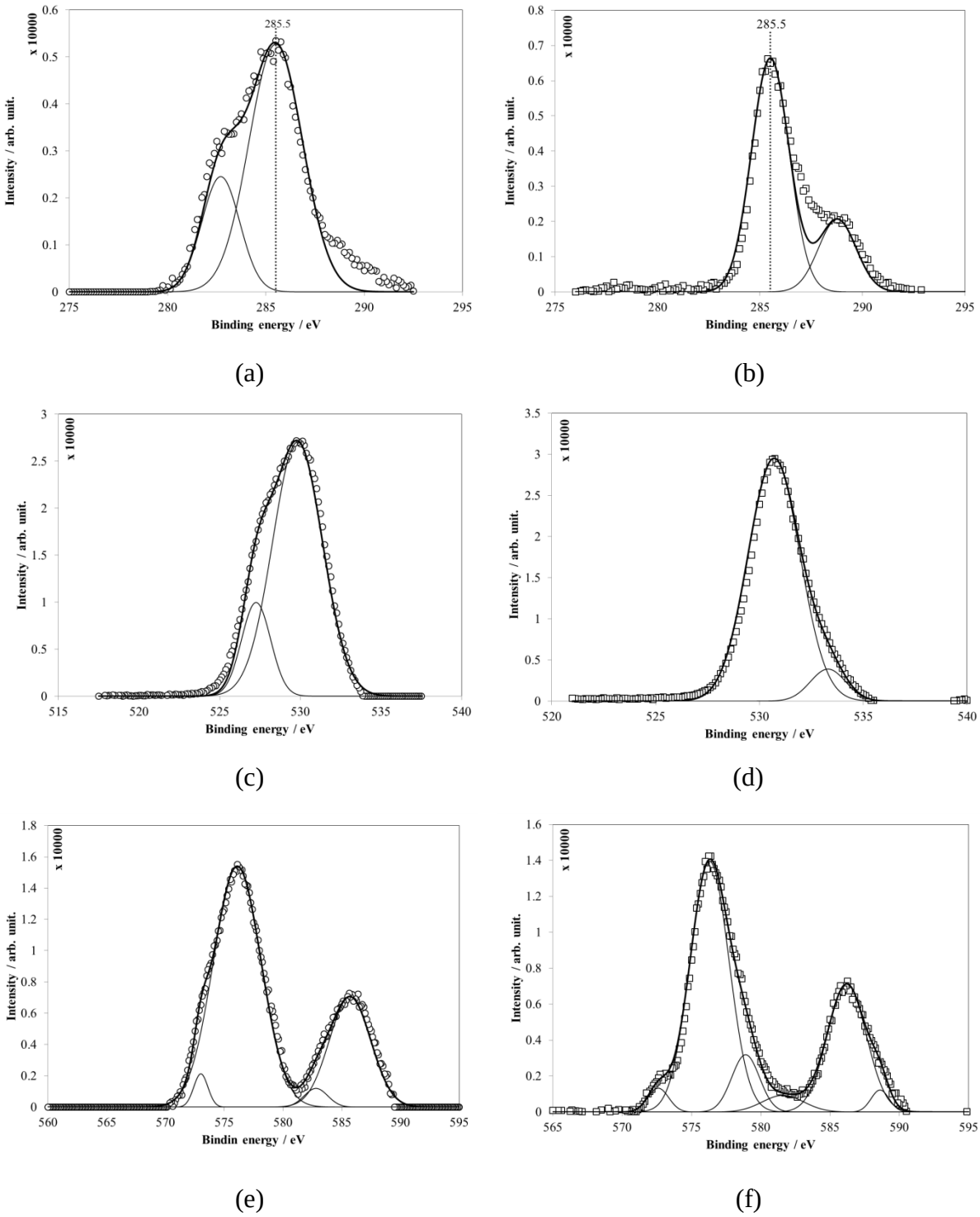

Figure S3 – X-ray photoelectron spectroscopy (XPS) analysis of Ti covered with $Cr(OH)_3$ or Cr_2O_3. a) C1s – Cr $(OH)_3$; b) O1s – Cr_2O_3; c) C1s – Cr $(OH)_3$; d) C1s – Cr_2O_3 e) Cr2p – $Cr(OH)_3$ and; f) Cr2p – Cr_2O_3.

Table 1 – Experimental and database binding energies of $Cr(OH)_3$ and Cr_2O_3.

Experimental	**O1s**	**Cr2p$_{3/2}$**	**Cr2p$_{1/2}$**
$Cr(OH)_3$	529.82	576.1	585.7
Cr_2O_3	530.70	576.3	585.7
Literature values*			
$Cr(OH)_3$	530.8 – 531.7	577.0 – 577.4	586.8
Cr_2O_3	529.8 – 530.8	576.1 – 580.1	586.0 – 586.4
Cr	-	573.8 – 574.7	583.5

*values obtained on-line at: http://srdata.nist.gov/xps/Default.aspx.

Figure S4 shows the Raman spectra of a Cr_2O_3@Ti electrode heat-treated at 900 ºC for 1 hour. After the heat treatment, the black Cr_2O_3 surface, gave place to a green, brittle layer, which was already an indication that the surface was converted to crystalline Cr_2O_3 [1]. The spectra were taken from the lowest (1% = 0.7 mW) to the highest (10% = 7.0 mW) laser power. The results demonstrate that the crystalline Cr_2O_3 phase is presented from the beginning, i.e., before phase transformation induced by light absorption.

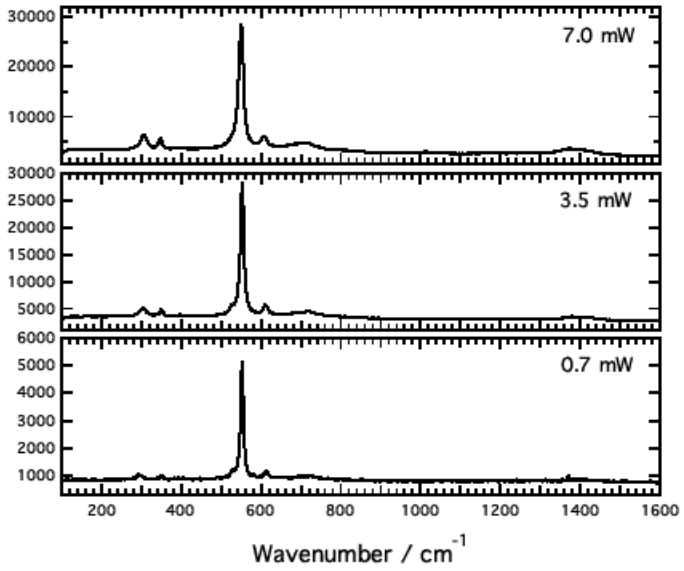

Figure S4 – Raman spectra of Cr_2O_3@Ti at different laser powers.

Figure S5 shows cyclic voltammograms using Ti rotating disc electrodes covered with $Cr(OH)_3$ (red line) or Cr_2O_3 (blue line). In the potential interval applied both surfaces showed good stability, and no further reduction or re-oxidation back to Cr(VI) is observed.

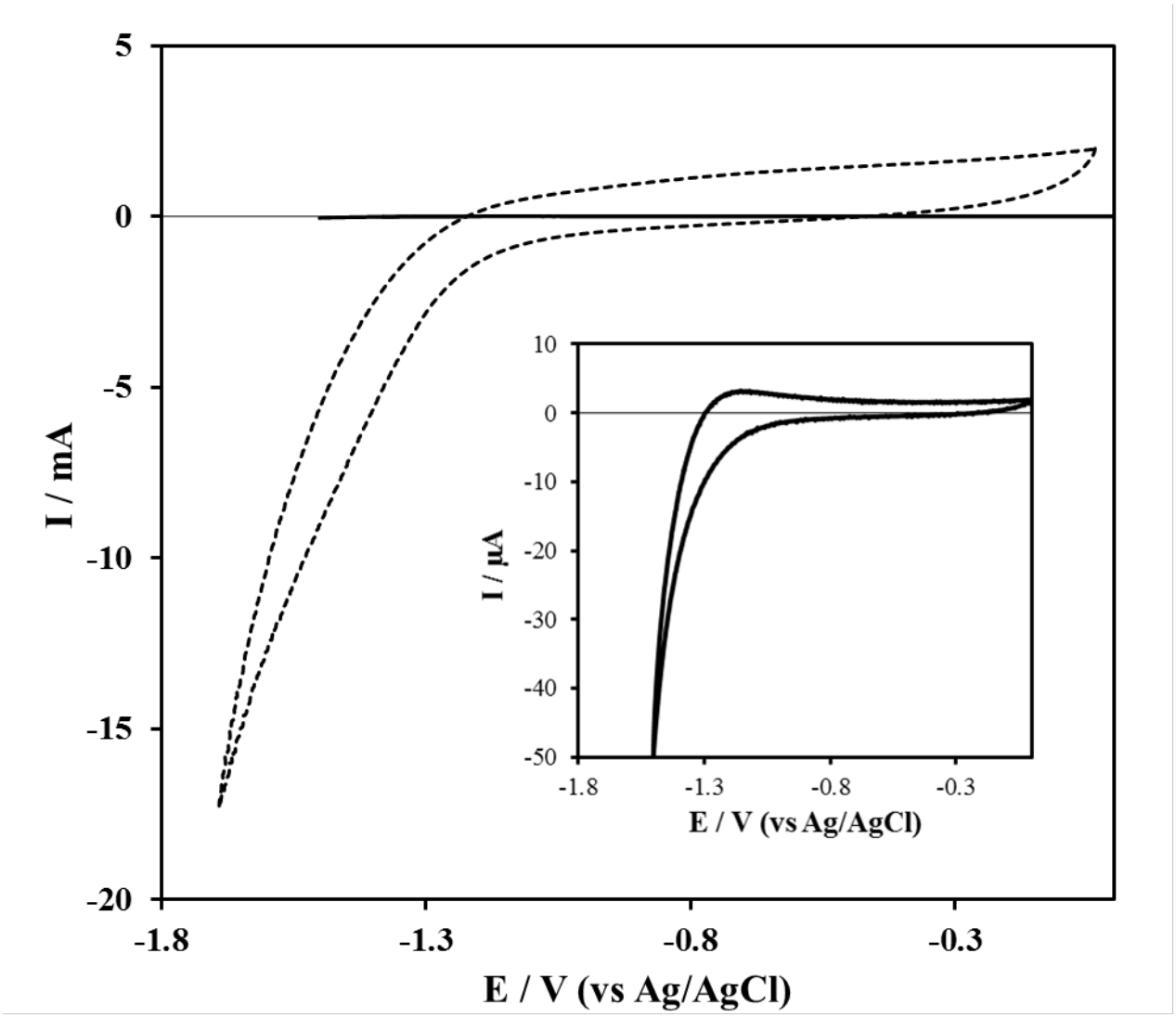

Figure S5 – Cyclic voltammetry of $Cr(OH)_3$@Ti (full line) and Cr_2O_3@Ti (broken line) in alkaline solution (Na_2SO_4 0.2 mol L^{-1}, pH 11). Sweep rate: 50 mV s^{-1}. The inset shows the voltammogram for $Cr(OH)_3$@Ti on the µA scale.

References

[1] S.-t. Liang, H.-l. Zhang, M.-t. Luo, K.-j. Luo, P. Li, H.-b. Xu, Y. Zhang, Ceramics International, 40 (2014) 4367-4373.